



Jacquard image segmentation using Mumford-Shah model*

FENG Zhi-lin (冯志林)^{†1,2}, YIN Jian-wei (尹建伟)², CHEN Gang (陈刚)², DONG Jin-xiang (董金祥)²

⁽¹⁾Department of Information and Engineering, College of Zhijiang, Zhejiang University of Technology, Hangzhou 310024, China)

⁽²⁾Department of Computer Science and Engineering, Zhejiang University, Hangzhou 310027, China)

[†]E-mail: fzlmailbox@21cn.com

Received May 18, 2005; revision accepted Dec. 19, 2005

Abstract: Jacquard image segmentation is one of the primary steps in image analysis for jacquard pattern identification. The main aim is to recognize homogeneous regions within a jacquard image as distinct, which belongs to different patterns. Active contour models have become popular for finding the contours of a pattern with a complex shape. However, the performance of active contour models is often inadequate under noisy environment. In this paper, a robust algorithm based on the Mumford-Shah model is proposed for the segmentation of noisy jacquard images. First, the Mumford-Shah model is discretized on piecewise linear finite element spaces to yield greater stability. Then, an iterative relaxation algorithm for numerically solving the discrete version of the model is presented. In this algorithm, an adaptive triangular mesh is refined to generate Delaunay type triangular mesh defined on structured triangulations, and then a quasi-Newton numerical method is applied to find the absolute minimum of the discrete model. Experimental results on noisy jacquard images demonstrated the efficacy of the proposed algorithm.

Key words: Mumford-Shah model, Image segmentation, Active contour, Variational method, Jacquard image
doi: 10.1631/jzus.2006.A0109 **Document code:** A **CLC number:** TP391

INTRODUCTION

Image segmentation plays an essential role in jacquard image analysis. A jacquard image consists of many complex patterns which contain detailed, intricate topological curves. An accurate extraction of pattern features from jacquard images promises reliability for jacquard fabric CAD. Although, many algorithms have been proposed for the segmentation problem, they have difficulty in capturing the complex structure of the visual features, such as complex contours of a jacquard pattern. In practice, the strong variability of jacquard patterns, and the low and varying contrast of topological curves in jacquard patterns make it quite difficult to obtain reliable performance with common segmentation methods.

Many active contour models (Kass *et al.*, 1988; Malladi *et al.*, 1995; Chesnaud *et al.*, 1999; Xiao *et al.*,

2003; Martin *et al.*, 2004) were proposed for extracting the contour of an object with a complex shape. However, in a jacquard image, consistently strong edge information is not always presented along the entire boundary of the contours to be segmented. Moreover, if the available jacquard image is heavily corrupted by noise, the performance of the active contour models is often inadequate.

Recently, these active contour models have been further improved by incorporating statistical model and prior knowledge to provide more accurate segmentation results. Chesnaud *et al.*(1999) proposed a probabilistic framework for image segmentation where different probability density functions from the exponential family are allowed. The parameters of the probability function are determined to deform the snake to detect the image regions. Zhuang *et al.*(1996) proposed a robust statistical approach for the problem of Gaussian mixture density modeling and decomposition. The approach can be incorporated into the statistical snake framework to achieve higher ro-

*Project (No. 2003AA411021) supported by the Hi-Tech Research and Development Program (863) of China

bustness for the shape detection from the noise data. Martin *et al.* (2004) analyzed level set implementation of region snakes based on maximum likelihood estimation techniques for different noise models belonging to the exponential family.

Mumford-Shah model (Mumford and Shah, 1989; Tsai *et al.*, 2001; Chen and Guan, 2004) is another popular method for complex pattern segmentation, which is more immune to noise than the active contour models and allows construction of more efficient strategies for detecting discontinuities in the presence of noise. In contrast to the active contour models, this method utilizes not only image information near the evolving contour but also image statistics inside and outside the contour, so it is more suitable for the segmentation of noisy jacquard images. In this paper, we focus on the segmentation of noisy jacquard images using the Mumford-Shah model.

However, the minimization of the Mumford-Shah model poses a difficult numerical problem, since it requires the computation of geometrical properties of the unknown set of discontinuity boundaries. There are many methods for the minimization of the model (Ambrosio and Tortorelli, 1990; Gobbino, 1998; Chambolle, 1995), but these methods are almost exclusively based on the steepest descent approach, which is not always the best approach for energy minimization.

In this paper, we propose an iterative relaxation algorithm to minimize the Mumford-Shah model on piecewise linear finite element spaces. Our algorithm involves two coordinate steps at each iteration: (1) refining and reorganizing an adaptive triangular mesh to characterize the essential contour structure of a pattern, and (2) minimizing the discrete version of the Mumford-Shah model by using the quasi-Newton algorithm.

THE MUMFORD-SHAH MODEL

Let $\Omega \subset \mathbb{R}^2$ be a bounded open set and $g \in L^\infty(\Omega)$ represent the image intensity. The function g has discontinuities that represent the contours of objects in the image. The image segmentation problem consists in the detection of such discontinuities with the simultaneous suppression of noise. Mumford and

Shah (1989) proposed a variational method for image segmentation which looks for a piecewise smooth approximation u of the function g , with u discontinuous across a closed set K . The variational problem consists in the minimization of the following functional

$$E(u, K) = \int_{\Omega \setminus K} |\nabla u|^2 dx + \alpha \int_{\Omega} (u - g)^2 dx + \beta H^1(K) \quad (1)$$

over closed set $K \subset \Omega$ and $u \in C^1(\Omega \setminus K)$. Here, H^1 is the one-dimensional Hausdorff measure, and α, β are positive weights. By the Mumford-Shah model, the image segmentation problem is then reduced to find a set K of contours decomposing the image into regions and a function u which is piecewise smooth on that decomposition. Here, the first term penalizes strong variations of u , thus ensuring that u is a smooth approximation of g , the second term forces u to be close to the given image g , and the last term prevents the edges from filling up the whole image.

WEAK FORMULATION AND Γ -CONVERGENCE

Heuristically, we expect solutions to Eq.(1) to be smooth and close to the image g at places $x \notin K$, and K constitutes edges of the image. To show existence of solutions to Eq.(1), a weak formulation was proposed by de Giorgi *et al.* (1990) by setting $K = S_u$ (the jumps set of u) and minimizing only over $u \in SBV$, the space of special functions of bounded variation. We recall some definitions and properties concerning functions with bounded variation.

Definition 1 Let $u \in L^1(\Omega; \mathbb{R}^2)$. We say that u is a function with bounded variation in Ω , and we write $u \in BV(\Omega; \mathbb{R}^2)$, if the distributional derivative Du of u is a vector-valued measure on Ω with finite total variation.

Definition 2 Let $u \in L^1(\Omega; \mathbb{R}^2)$. We denote by S_u the complement of the Lebesgue set of u , i.e., $x \notin S_u$ if and only if $\lim_{\rho \rightarrow 0} \rho^{-n} \int_{B_\rho(x)} |u(y) - z| dy = 0$ for some $z \in \mathbb{R}^2$, where $B_\rho(x) = \{y \in \mathbb{R}^2: |y-x| < \rho\}$.

Definition 3 Let $u \in BV(\Omega)$. We define the three measures $D^a u$, $D^j u$ and $D^c u$ as follows.

By the Radon-Nikodym theorem we set $Du = D^a u + D^s u$ where $D^a u$ is the absolutely continuous part

of Du , $D^s u$ is the singular part of Du . $D^s u$ can be further decomposed into the part supported on S_u (the jump part $D^j u$) and the rest (the Cantor part $D^c u$): $D^j u = D^s u|_{S_u}$ and $D^c u = D^s u|_{\Omega \setminus S_u}$. Thus, we can then write $Du = D^a u + D^j u + D^c u$.

Definition 4 Let $u \in BV(\Omega)$. We say that u is a special function of bounded variation, and we write $u \in SBV(\Omega)$, if $D^c u = 0$.

De Giorgi et al.(1990) gave the weak formulation of the original problem Eq.(1) as follows:

$$E(u) = \int_{\Omega} |\nabla u|^2 dx + \alpha \int_{\Omega} (u - g)^2 dx + \beta H^1(S_u). \quad (2)$$

They also proved that minimizers of the weak problem Eq.(2) are minimizers of the original problem Eq.(1). However, from a numerical point of view, it is not easy to compute a minimizer for Eq.(2), due to the term $H^1(S_u)$, and to the fact that this functional is not lower-semicontinuous with respect to S_u . It is natural to try to approximate Eq.(2) by simpler functionals defined on SBV spaces. Ambrosio and Tortorelli (1990) showed that Eq.(2) can be approximated by a sequence of elliptic functionals which are numerically more tractable. The approximation takes place in the sense of Γ -convergence.

To approximate and compute solutions to Eq.(2), the most popular and successful approach is to use the theory of Γ -convergence. This theory, introduced by de Giorgi and Franzoni (dal Maso, 1993), is designed to approximate a variational problem by a sequence of regularized variational problems which can be solved numerically by finite difference/finite element methods. Note that Γ -convergence is stable under continuous perturbations, and guarantees the convergence of minima and minimizers.

Definition 5 Let X be a metric space, let $\{F_k\}$ be a sequence of functions defined in X with values in \mathbb{R} .

Let us set

$$\Gamma\text{-}\limsup_{k \rightarrow +\infty} F_k(u) := \inf_{u_k \rightarrow u} \left\{ \liminf_{k \rightarrow +\infty} F_k(u_k) : \{u_k\} \rightarrow u \right\},$$

$$\Gamma\text{-}\liminf_{k \rightarrow +\infty} F_k(u) := \inf_{u_k \rightarrow u} \left\{ \limsup_{k \rightarrow +\infty} F_k(u_k) : \{u_k\} \rightarrow u \right\}.$$

If $\Gamma\text{-}\liminf_{k \rightarrow +\infty} F_k(u) = \Gamma\text{-}\limsup_{k \rightarrow +\infty} F_k(u) = F(u)$ for all $x \in X$,

we say that F is the Γ -limit of $\{F_k\}$, and we write

$$F(x) = \Gamma\text{-}\lim_{k \rightarrow +\infty} F_k(x).$$

Theorem 1 Assume F_k Γ -converges to F and for every k , let u_k be a minimizer of F_k over X . If the sequence (or a subsequence) u_k converges to some $u \in X$, then u is a minimizer for F and $F_k(u_k)$ converges to $F(u)$.

So, we say that a family $\{F_{\varepsilon}\}_{\varepsilon > 0}$ of functions Γ -converges to F as $\varepsilon \rightarrow 0^+$, if $\{F_{\varepsilon}\}$ Γ -converges to F for every sequence $\{\varepsilon_j\} \rightarrow 0^+$.

DISCRETE FUNCTIONAL OF NUMERICAL APPROXIMATION

Now we consider the numerical approximation, in the sense of Γ -convergence, by a sequence of discrete functionals defined on finite elements spaces over structured and adaptive triangulation.

Let $\Omega = (0,1) \times (0,1)$, let $T_{\varepsilon}(\Omega)$ be the triangulations and let ε denote the greatest length of the edges in the triangulations. Moreover let $V_{\varepsilon}(\Omega)$ be the finite element space of piecewise affine functions on the mesh $T_{\varepsilon}(\Omega)$, let $\{T_{\varepsilon_j}\}$ be a sequence of triangulations with $\varepsilon_j \rightarrow 0$ and let $f: [0, +\infty) \rightarrow [0, +\infty)$ be a non-decreasing continuous function such that $\lim_{t \rightarrow 0} \frac{f(t)}{t} = 1$ and

$$\lim_{t \rightarrow +\infty} f(t) = f_{\infty} < +\infty.$$

Negri (1999) proved the following theorem.

Theorem 2 For each sequence of triangulations $\{T_{\varepsilon_j}\}$ there exists a convex, 1-homogeneous function $\phi: \mathbb{R}^2 \rightarrow [0, +\infty)$ such that the functional

$$F_{\varepsilon_j}(u, T) = \frac{1}{\varepsilon_j} \int_{\Omega} f(\varepsilon_j |\nabla u_T|^2) dx + \int_{\Omega} (u_T - g)^2 dx. \quad (3)$$

Γ -converges with respect to strong L^2 -topology to the anisotropic Mumford-Shah model

$$F(u) = \int_{\Omega} (|\nabla u|^2 + (u - g)^2) dx + f_{\infty} \int_{S_u} \phi(v_u) dH^1, \quad (4)$$

where $u \in V_{\varepsilon}(\Omega)$, $T \in T_{\varepsilon}(\Omega)$, $u_T \in V_{\varepsilon}(\Omega) \times T_{\varepsilon}(\Omega)$.

We choose $f(x) = (2\beta/\pi) \arctan(\pi x/2\beta)$, and define the minimizing discrete model as follows:

$$F_{\varepsilon_j}(u, T) = \alpha \int_{\Omega} (u_T - g)^2 dx + \frac{1}{\varepsilon_j} \int_{\Omega} \frac{2\beta}{\pi} \arctan \left(\frac{\pi \varepsilon_j}{2\beta} |\nabla u_T|^2 \right) dx. \quad (5)$$

By Theorem 2, we know that Eq.(5) Γ -converges to

$$F(u) = \alpha \int_{\Omega} |u - g|^2 dx + \int_{\Omega} |\nabla u|^2 dx + \beta \int_{S_u} \phi(v_u) dH^1, \quad (6)$$

where v_u is a unit normal to S_u . Eq.(6) is an anisotropic version of Eq.(2), and the function ϕ is applied to take into account the anisotropy introduced by the geometry of the triangulation T .

NUMERICAL IMPLEMENTATION

In order to arrive at the joint minimum (u, T) of Eq.(5), we propose an iterative relaxation algorithm to implement the numerical solving of Eq.(5). The main idea of the proposed algorithm is as follows: alternating back and forth between minimizing Eq.(5) holding T constant and adapting triangulation T holding u constant.

The intuitive idea behind the algorithm is that if the triangulation T were known and held constantly, it would be straightforward to calculate the variable u , and the triangulation T can be straightforwardly calculated if the variable u were known. At each iteration, a scheme for the mesh adaptation is first enforced to refine and reorganize a triangular mesh to characterize the essential contour structure. Then, the quasi-Newton algorithm is applied to find the absolute minimum of the discrete functional. Fig.1 is the outline of the proposed algorithm.

Mesh adaptation algorithm

There are several approaches to refine and reorganize an existing triangulation. Delaunay triangulation algorithms have been used successfully for unstructured mesh generation. In this paper, we use the Delaunay type mesh generator BL2D (Borouchaki and Laug, 1996) to make the triangular mesh accurately characterize the essential contour structure.

BL2D is a bidimensional, adaptive and anisot-

1. Initialize iteration index: $j \leftarrow 0$;
2. Set initial ε_j and u_j ;
3. Generate the adapted triangulation T_{ε_j} by the mesh adaptation algorithm, according to u_j ;
4. Minimize $F_{\varepsilon_j}(u_j)$ on the triangulation T_{ε_j} by the quasi-Newton minimizing algorithm;
5. Update the current index: $j \leftarrow j+1$;
6. Generate a new ε_j ;
7. If $|\varepsilon_j - \varepsilon_{j-1}| > \mu$, return to Step 3. Otherwise, goto Step 8;
8. Stop.

Fig.1 Outline of the proposed algorithm

ropic mesh generator. It uses the Delaunay's method to generate a triangular mesh. In BL2D, the background mesh is an existing mesh applied to generate an adaptive foreground mesh. The foreground mesh is built from the background mesh by an estimator which consists of giving a metric at each point of the background mesh. The metric is represented by a symmetric positive definite matrix with three coefficients (a, b, c) . By a rotation at an angle θ making a reference line parallel to one of the two axes of the ellipse, the metric (a, b, c) is easily obtained by the relation

$$\begin{pmatrix} a & b \\ b & c \end{pmatrix} = \begin{pmatrix} \cos \theta & -\sin \theta \\ \sin \theta & \cos \theta \end{pmatrix} \times \begin{pmatrix} 1/h_1^2 & 0 \\ 0 & 1/h_2^2 \end{pmatrix} \times \begin{pmatrix} \cos \theta & \sin \theta \\ -\sin \theta & \cos \theta \end{pmatrix},$$

where the values h_1 and h_2 represent the desired sizes along two orthogonal directions. As the three quantities (θ, h_1, h_2) are related to the orientation and anisotropy factor of the elements in the adapted triangulation, we can enforce an adaptation of the triangular mesh as follows: (1) setting three quantities according to the function u obtained from the minimizing component at the previous iteration, and (2) building the foreground mesh as a Delaunay triangulation with respect to the metric which is given at each point of the background triangulation, according to the above three quantities. The interested reader can refer to the book (George and Borouchaki, 1998) for detailed description of the building of the adaptive mesh.

The minimizing algorithm

Once a triangulation T is given, we need to minimize $F_\varepsilon(u)$ with respect to u , which is piecewise linear on each element of T and continuous on Ω . In general, standard minimizing techniques may fail due both to the lack of convexity and to the presence of many local minima. In order to ensure that the energy decreases at each iteration, we apply the quasi-Newton algorithm to minimize $F_\varepsilon(u)$. The quasi-Newton algorithm is the most popular algorithms in nonlinear optimization, with a reputation for fast convergence. The most widely used quasi-Newton formula is BFGS, which preserves the symmetry and positive definiteness of the approximation of the Hessian matrix, which may be satisfied with a line search using the Wolfe condition. In this paper, we use BFGS formula to approximate the Hessian matrix. Fig.2 shows a flowchart of the minimizing algorithm for the functional $F_\varepsilon(u)$.

1. Initialize step index: $k \leftarrow 0$;
2. Compute the gradient $\nabla F_\varepsilon(u_k)$ and the Hessian approximation matrix $\tilde{\nabla}^2 F_\varepsilon(u_k)$;
3. If $\nabla F_\varepsilon(u_k) = 0$, get a minimizer u_k and goto Step 9;
4. Compute a preconditioner for $\tilde{\nabla}^2 F_\varepsilon(u_k)$ with incomplete Cholesky factorization to preserve the sparsity of the original matrix;
5. Compute the descent direction d_k by the linear system $\tilde{\nabla}^2 F_\varepsilon(u_k) = -\nabla F_\varepsilon(u_k)$;
6. Compute the optimum step t_k along d_k by minimizing the 1-dimensional restriction of $F(u_k)$ to the interval $\{u_k + td_k\}$ for $t \in [0, 1]$;
7. Update the current index: $k \leftarrow k + 1$;
8. If $|u_k - u_{k-1}| < \gamma$, return to Step 2. Otherwise, goto Step 9.
9. Stop.

Fig.2 The minimizing algorithm

EXPERIMENTAL RESULTS

In this section, we carry out some experiments respectively on a synthetic image (256×256 pixels), and three jacquard images (256×256 pixels) with different types of contours and shapes. The results were obtained using software written in C programming language on the UNIX operating system running on an IPC SUN workstation. In our numerical experiments, we chose the parameters as follows: $\alpha=0.1, \beta=0.001, \gamma=2.5 \times 10^{-2}, \mu=3.125 \times 10^{-4}, \varepsilon=1/256 \approx 0.004$. As in practice it is difficult to exactly determine the noise in real images, here we examine the performance of our algorithm by adding “salt and pepper” noise to all the tested images. First, we obtain the initial background mesh by BL2D software. Then, we generate the initial adapted triangulation T_0 by the mesh adaptation algorithm according to the original image function u_0 . Fig.3 illustrates the above segmentation process of a synthetic image. Fig.3a gives a synthetic image u_0 with 40% noise. Fig.3b gives the initial background mesh generated by BL2D. After 8 mesh adaptation processes, the final foreground mesh T_7 is shown in Fig.3c. The segmented image and its edge set are shown in Figs.3d and 3e.

We measure the order of accuracy of the mesh adaptation algorithm by comparing the length and area error of the triangular-shape in Fig.3a between the analytical solution and numerical solution. Table 1 provides detailed accuracy measurements. It shows how the length error, area error, the three quantities (θ, h_1, h_2) , and the three coefficients (a, b, c) of the symmetric positive definite matrix depend on the mesh size ε . As the mesh size decreases, the adaptive triangular mesh will be more and more approaching the boundary of the triangular-shape.

We also conducted experiments to compare our

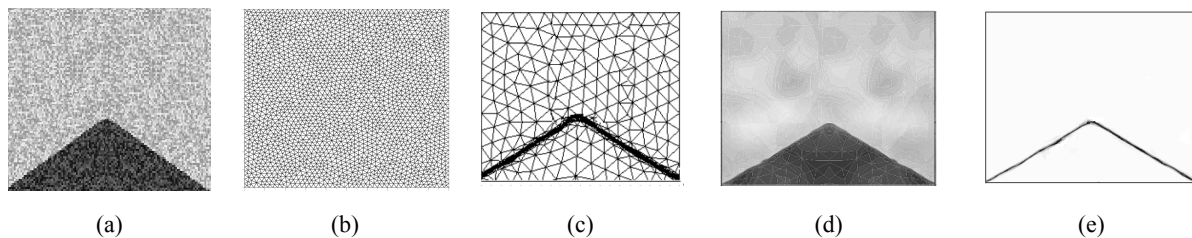


Fig.3 Segmentation of a synthetic image with 40% noise. (a) Noisy synthetic image; (b) Initial background mesh; (c) Final foreground mesh; (d) Segmented image; (e) Edge set

algorithm with a traditional active contours algorithm, the geometric active contours algorithm (Malladi *et al.*, 1995) under different noise environments. Fig.4 and Fig.5 illustrate the segmentation results of three jacquard images using the geometric active contours

(GAC) algorithm and our algorithm, respectively. We select three images with different shapes of petals from our jacquard image database. The shapes of petals in Figs.4a~4c are roundish, cuspidate and irregular, respectively. Figs.5a~5c show the segmenta-

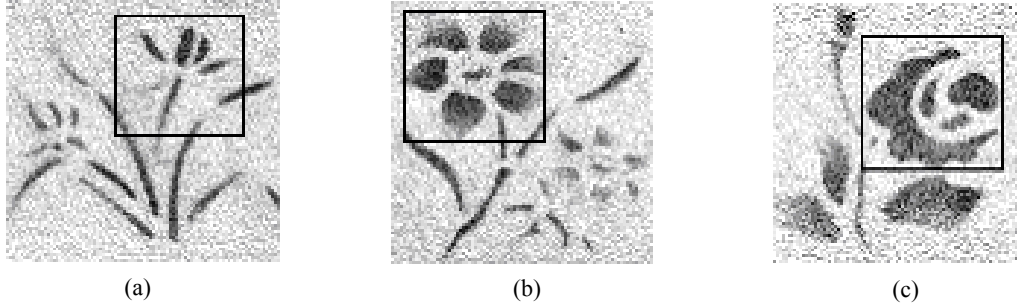


Fig.4 Three shapes of petals with 40% noise. (a) Roundish; (b) Cuspidate; (c) Irregular

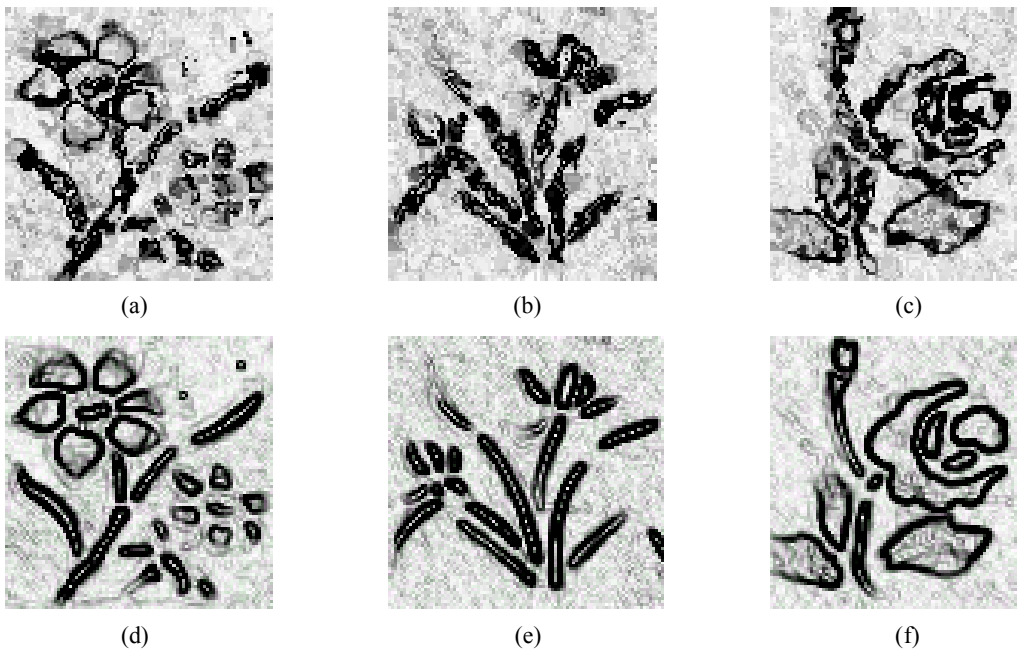


Fig.5 Segmentation results of jacquard images using two different algorithms. (a)~(c) and (d)~(f) are segmentation results using GAC algorithm and our algorithm, respectively

Table 1 Number of length and area error changes during the mesh adaptation processes

Mesh size (ϵ)	Length error	Area error	θ	h_1	h_2	a	b	c
0.004	0.05400	0.007300	42.34	3.230	3.483	0.08976	0.00668	0.08851
0.002	0.02800	0.003600	42.56	3.452	3.463	0.08367	0.00026	0.08363
0.001	0.00870	0.000940	43.68	3.479	3.498	0.08219	0.00044	0.08215
0.0005	0.00450	0.000450	43.73	3.485	3.491	0.08220	0.00014	0.08218
0.00025	0.00180	0.000260	44.54	3.469	3.521	0.08190	0.00121	0.08186
0.000125	0.00094	0.000160	44.92	3.488	3.538	0.08104	0.00115	0.08103
0.0000625	0.00034	0.000083	45.04	3.495	3.541	0.08080	0.00105	0.08081
0.00003125	0.00018	0.000045	45.17	3.450	3.553	0.08160	0.00240	0.08163

ϵ is the greatest length of the edges in the triangulation

tion results of jacquard images in Fig.4 using the GAC algorithm. Figs.5d~5f show the segmentation results of jacquard images in Fig.4 using our algorithm after 10 mesh adaptation processes. Comparing with Figs.5a~5c, sharp boundaries are accurately detected and strengthened in Figs.5d~5f. They clearly demonstrate the sturdiness of our algorithm when subject to noise. Analysis of the experiment results showed that false detected or missed boundaries are mainly caused by noise occurring on the boundaries, which confuses the detection of boundaries by the GAC algorithm. This experiment also showed how our algorithm can be applied to detect edges or other features in contours without gradients, while it is impossible for the GAC algorithm based on the gradient information. Here, we can see that our algorithm is more robust than the GAC algorithm for the segmentation of noise-corrupted jacquard images. Fig.6 shows the triangular meshes of the pedals in Figs.5d~5f which are generated by BL2D.

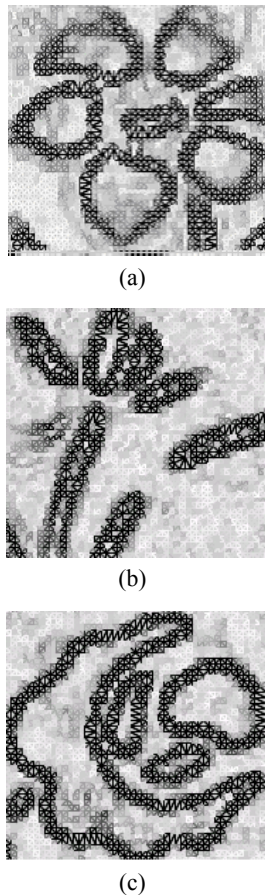


Fig.6 Triangular mesh generated by BL2D

In Fig.7, we give 3D plots of the segmented petals in Fig.4 using two different algorithms. It can be seen clearly that our algorithm is more suitable for the preservation of topological shapes of petals under noisy environment.

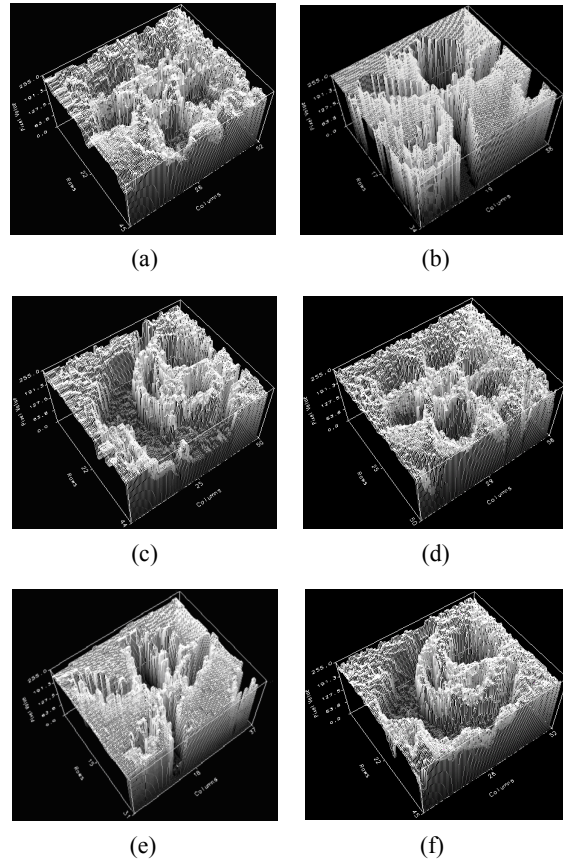


Fig.7 Comparison of segmentation results with 40% noise. (a)~(c) GAC algorithm; (d)~(f) Our algorithm

CONCLUSION

In summary, we have presented a novel algorithm for jacquard image segmentation based on the Mumford-Shah model. For solving the corresponding minimization problem, an iterative relaxation algorithm is proposed. The proposed algorithm is applied to segment noisy jacquard images and shows its capability of accurate segmentation. Experimental results showed that the proposed algorithm enhances its resistance to noise, so that the drawback of the active contour methods being easily affected by noise is greatly reduced. Future work would look into learning

patterns of variability from a training set and exploiting prior knowledge to provide more robust and accurate results.

References

- Ambrosio, L., Tortorelli, V.M., 1990. Approximation of functionals depending on jumps by elliptic functionals via Gamma-convergence. *Comm. Pure Appl. Math.*, **43**:999-1036.
- Borouchaki, H., Laug, P., 1996. The BL2D Mesh Generator: Beginner's Guide, User's and Programmer's Manual. Technical Report RT-0194, INRIA.
- Chambolle, A., 1995. Image segmentation by variational methods: Mumford and Shah functional and the discrete approximations. *SIAM J. Appl. Math.*, **55**(3):827-863. [doi:10.1137/S0036139993257132]
- Chen, X.F., Guan, Z.C., 2004. Image segmentation based on Mumford-Shah functional. *Journal of Zhejiang University SCIENCE*, **5**(1):123-128. [doi:10.1631/jzus.2004.0123]
- Chesnaud, C., Refregier, P., Boulet, V., 1999. Statistical region snake-based segmentation adapted to different physical noise models. *IEEE Trans. Pattern Analysis and Machine Intelligence*, **21**(11):1145-1157. [doi:10.1109/34.809108]
- dal Maso, G., 1993. An Introduction to Γ -Convergence. Birkhäuser, Boston.
- de Giorgi, E., Carriero, M., Leaci, A., 1990. Existence theorem for a minimum problem with free discontinuity set. *Arch. Rational Mech. Anal.*, **111**(4):291-322. [doi:10.1007/BF00376024]
- George, P.L., Borouchaki, H., 1998. Delaunay Triangulation and Meshing: Application to Finite Elements. Hermes, Paris.
- Gobbino, M., 1998. Finite difference approximation of the Mumford-Shah functional. *Comm. Pure Appl. Math.*, **51**(2):197-228. [doi:10.1002/(SICI)1097-0312(199802)51:2<197::AID-CPA3>3.0.CO;2-6]
- Kass, M., Witkin, A., Terzopoulos, D., 1988. Snakes: Active contour models. *Int. J. Computer Vis.*, **1**(4):321-331. [doi:10.1007/BF00133570]
- Malladi, R., Sethian, J.A., Vemuri, B.C., 1995. Shape modeling with front propagation: A level set approach. *IEEE Trans. Pattern Analysis and Machine Intelligence*, **17**(2):158-175. [doi:10.1109/34.368173]
- Martin, P., Goudail, F., Refregier, P., Guerauld, F., 2004. Influence of the noise model on level set active contour segmentation. *IEEE Trans. Pattern Analysis and Machine Intelligence*, **26**(6):799-803. [doi:10.1109/TPAMI.2004.11]
- Mumford, D., Shah, J., 1989. Optimal approximations by piecewise smooth functions and associated variational problems. *Comm. Pure Appl. Math.*, **42**(5):577-685.
- Negri, M., 1999. The anisotropy introduced by the mesh in the finite element approximation of the Mumford-Shah Functional. *Numer. Funct. Anal. Optim.*, **20**:957-982.
- Tsai, A., Yezzi, A.Jr., Willsky, A.S., 2001. Curve evolution implementation of the Mumford-Shah Functional for image segmentation, denoising, interpolation, and magnification. *IEEE Trans. Image Processing*, **10**(8):1169-1186. [doi:10.1109/83.935033]
- Xiao, H., Xu, C.Y., Prince, J.L., 2003. A topology preserving level set method for geometric deformable models. *IEEE Trans. Pattern Analysis and Machine Intelligence*, **25**(6):755-768. [doi:10.1109/TPAMI.2003.1201824]
- Zhuang, X.H., Huang, Y., Palaniappan, K., Zhao, Y.X., 1996. Gaussian mixture density modeling, decomposition, and applications. *IEEE Trans. Image Processing*, **5**(9):1293-1302. [doi:10.1109/83.535841]

Welcome visiting our journal website: <http://www.zju.edu.cn/jzus>

Welcome contributions & subscription from all over the world

The editor would welcome your view or comments on any item in the journal, or related matters

Please write to: Helen Zhang, Managing Editor of JZUS

E-mail: jzus@zju.edu.cn Tel/Fax: 86-571-87952276/87952331